Ventilation of the abyssal Southern Ocean during the late Neogene: A new perspective from the subantarctic Pacific

Lindsey M. Waddell,[1,2] Ingrid L. Hendy,[1] Theodore C. Moore,[1] and Mitchell W. Lyle[3]

Received 16 July 2008; revised 24 May 2009; accepted 10 June 2009; published 19 August 2009.

[1] Benthic foraminiferal stable carbon isotope records from the South Atlantic show significant declines toward more "Pacific-like" values at ~7 and ~2.7 Ma, and it has been posited that these shifts may mark steps toward increased CO_2 sequestration in the deep Southern Ocean as climate cooled over the late Neogene. We generated new stable isotope records from abyssal subantarctic Pacific cores MV0502-4JC and ELT 25-11. The record from MV0502-4JC suggests that the Southern Ocean remained well mixed and free of vertical or interbasinal $\delta^{13}C$ gradients following the late Miocene carbon shift (LMCS). According to the records from MV0502-4JC and ELT 25-11, however, cold, low $\delta^{13}C$ bottom waters developed in the Southern Ocean in the late Pliocene and persisted until ~1.7 Ma. These new data suggest that while conditions in the abyssal Southern Ocean following the LMCS were comparable to the present day, sequestration of respired CO_2 may have increased in the deepest parts of the Southern Ocean during the late Pliocene, a critical period for the growth and establishment of the Northern Hemisphere ice sheets.

Citation: Waddell, L. M., I. L. Hendy, T. C. Moore, and M. W. Lyle (2009), Ventilation of the abyssal Southern Ocean during the late Neogene: A new perspective from the subantarctic Pacific, *Paleoceanography*, *24*, PA3206, doi:10.1029/2008PA001661.

1. Introduction

[2] In seeking the mechanism behind the glacial-interglacial atmospheric CO_2 variations of the past two million years, many researchers have pointed to the potential of the Southern Ocean for storing and releasing significant quantities of CO_2 in the form of dissolved inorganic carbon (DIC). Traditionally, changes in Southern Ocean biology have been one of the most frequently invoked mechanisms for explaining low glacial atmospheric CO_2 levels, but recent study suggests that changes in the marine biological pump can account for less than half of the observed glacial-interglacial variation [*Kohfeld et al.*, 2005]. In the past decade, many researchers have come to an understanding that the circulation of the Southern Ocean was fundamentally different during the Pleistocene glaciations than at present, and thus many physical mechanisms for sequestering CO_2 within the glacial Southern Ocean have been proposed. In the modern ocean, the upwelling of Circumpolar Deepwater at the Antarctic Divergence is the primary mechanism by which waters deeper than 2500 m are exposed to the atmosphere, and with this exposure, CO_2 respired at depth can be released. During glacial periods, however, ventilation of these deep waters may have been inhibited by physical changes such as increased surface water stratification [*Francois et al.*, 1997; *Sigman et al.*, 1999, 2004; *Jaccard et al.*, 2005; *Brunelle et al.*, 2007; *de Boer et al.*, 2007; *Sigman et al.*, 2007], increased sea ice cover [*Stephens and Keeling*, 2000; *Adkins et al.*, 2002], and decreased upwelling [*Toggweiler et al.*, 2006; *Watson and Naveira Garabato*, 2006].

[3] In the Atlantic sector of the Southern Ocean, glacial intervals since 1.55 Ma have been characterized by benthic $\delta^{13}C$ values that are consistently lower than those of the glacial Pacific Ocean [*Hodell et al.*, 2003; *Hodell and Venz-Curtis*, 2006]. This suggests that the buildup and subsequent release of respired CO_2 from the deep Atlantic sector of the Southern Ocean may have influenced atmospheric CO_2 on glacial-interglacial timescales. While the low benthic $\delta^{13}C$ values attained in the deep South Atlantic during glacial intervals after 1.55 Ma may appear to be a Pleistocene phenomenon, these may actually be part of a larger trend of decreasing $\delta^{13}C$ values over the last 9 Ma that occurred in two main steps. The first of these declines coincides with the late Miocene carbon shift (LMCS) at ~7 Ma. Although this decrease in benthic $\delta^{13}C$ has been identified in foraminiferal records throughout the world's oceans [*Haq et al.*, 1980], its magnitude appears greatest in records from the South Atlantic [*Hodell and Venz-Curtis*, 2006]. The second shift occurred at ~2.7 Ma during the late Pliocene climate transition (LPCT) and has been identified only in benthic $\delta^{13}C$ records from >2500 m depth in the Atlantic sector of the Southern Ocean [*Hodell and Venz*, 1992; *Hodell et al.*, 2002; *Hodell and Venz-Curtis*, 2006]. Because both the LMCS and the LPCT were associated with shifts in interbasinal $\delta^{13}C$ gradients in which carbon isotope values in the South Atlantic became increasingly Pacific-like, it has been posited that these carbon events may mark steps toward increased CO_2 sequestration in the deep Southern Ocean as high-latitude climate cooled over the late Neogene [*Hodell and Venz-Curtis*, 2006].

[1]Department of Geological Sciences, University of Michigan, Ann Arbor, Michigan, USA.
[2]Now at Department of Geology, Grand Valley State University, Allendale, Michigan, USA.
[3]Department of Oceanography, Texas A&M University, College Station, Texas, USA.

0883-8305/09/2008PA001661

[4] In fact, evidence now suggests that many of the physical mechanisms that likely hindered the release of respired CO_2 from the deep Southern Ocean during the glaciations of the late Quaternary were operating by the late Pliocene. While the Northern Hemisphere ice sheets were still in their infancy, Antarctica appears to have been reaching an advanced state of glaciation that was accompanied by changes in the circulation of the Southern Ocean. A strong halocline developed in the Antarctic and subarctic Pacific coincident with the onset of Northern Hemisphere Glaciation at 2.73 Ma [*Haug et al.*, 1999; *Sigman et al.*, 2004], and Antarctic sea ice expanded to the South Orkney microcontinent by 2.5–2.4 Ma [*Burckle et al.*, 1990; *Kennett and Barker*, 1990]. Most importantly, a decline in atmospheric pCO_2 to preindustrial levels may have been a requirement for the initiation of ice sheets in the Northern Hemisphere [*Lunt et al.*, 2008], and the decline in benthic $\delta^{13}C$ in the deep South Atlantic (>2500 m) at ~2.7 Ma suggests that a consequence of this late Pliocene expansion of the Antarctic cryosphere may have been increased sequestration of CO_2 within the deep Southern Ocean [*Hodell and Venz-Curtis*, 2006].

[5] Unfortunately, our current knowledge of carbon isotope changes in the Southern Ocean during the late Neogene is based almost entirely on stable isotope records from sediment cores recovered from the South Atlantic region. Thus, while *Hodell and Venz-Curtis* [2006] have shown that the LMCS and LPCT were associated with shifts in interbasinal $\delta^{13}C$ gradients between the North Atlantic, South Atlantic, and equatorial Pacific Oceans, the nature, or in the case of the LPCT, even the existence, of these shifts in the Pacific sector of the Southern Ocean has remained largely unknown. Herein we offer new stable isotope records from two piston cores obtained from the depths of approximately 4000 m or greater in the subantarctic Pacific region. These records are significant not only because they provide a circum-Antarctic perspective for the carbon isotope shifts associated with the LMCS and LPCT, but also because they are among the deepest stable isotope records yet available from the late Neogene Southern Ocean.

2. Background

2.1. Using $\delta^{13}C$ to Reconstruct Changes in Deepwater Circulation

2.1.1. Controls on the $\delta^{13}C$ of Deepwater

[6] Carbon isotopes are a valuable water mass tracer in the study of deepwater circulation patterns. In large part because of the role of biologic productivity in the distribution of carbon isotopes in the ocean, deep water masses can acquire distinct $\delta^{13}C$ values that can be used to discern their source region and/or age. Prior to sinking, deep waters obtain a preformed $\delta^{13}C$ value that is reflective of productivity and air-sea exchange processes in their source region.

[7] Deepwater sourced from surface water in which productivity and/or nutrient utilization is high will have a high $\delta^{13}C$ value and a low nutrient concentration compared to deepwater sourced in regions of low productivity/nutrient utilization. In the modern ocean, North Atlantic Deepwater (NADW) has $\delta^{13}C$ values between 1.0 and 1.5‰ because of high nutrient utilization in its source waters, which originate in the subtropics above a strong thermocline, whereas Antarctic Bottom Water (AABW) has an average $\delta^{13}C$ value of 0.3‰ because of nutrient underutilization near Antarctica [*Kroopnick*, 1985].

[8] The preformed $\delta^{13}C$ value of deepwater is also influenced by the isotopic equilibration of atmospheric CO_2 with DIC in the surface water mass. Air-sea exchange in the source region acts to increase the preformed $\delta^{13}C$ value of the water mass under colder temperatures and lower it under warmer temperatures, but the residence time of the water at the air-sea interface is usually shorter than the time required to reach isotopic equilibrium. Thus, the influence of air-sea exchange is usually highest in areas where wind speeds are high, such as the modern subantarctic, where planktonic foraminifera record a $\delta^{13}C$ enrichment of up to 1‰ [*Charles and Fairbanks*, 1990; *Broecker and Maier-Reimer*, 1992; *Lynch-Stieglitz et al.*, 1995; *Ninnemann and Charles*, 1997].

[9] As deepwater circulates within the ocean, its $\delta^{13}C$ value evolves as it mixes with other water masses and "ages." Aging occurs as the water mass accumulates ^{12}C from the oxidation of sinking organic matter. The most nutrient-rich water ($\delta^{13}C \approx 0$) in today's ocean is found at middepth (~2000 m) in the North Pacific, where nutrients become "trapped" as deepwater upwells at the end of the deepwater conveyor [*Matsumoto et al.*, 2002].

2.1.2. Benthic Foraminifera as a Recorder of Deepwater $\delta^{13}C$

[10] The carbon isotopic composition of benthic foraminifera is considered a reliable recorder of the $\delta^{13}C$ value of DIC in the surrounding water mass and thus is commonly used in the reconstruction of past deepwater chemistry and circulation. Interspecies differences in microhabitat and vital effects can result in a consistent $\delta^{13}C$ offset between many modern species of foraminifera and calcite precipitated in equilibrium with seawater. In general, however, epifaunal foraminifera such as *Planulina* and *Cibicidoides* spp., more closely record bottom water $\delta^{13}C$ values than infaunal species, which often exhibit lower $\delta^{13}C$ values reflective of the decomposition of organic matter in the pore waters [*McCorkle et al.*, 1990].

[11] In areas with high surface water productivities, it is possible for the $\delta^{13}C$ value of epifaunal benthic foraminifera to show a negative offset of up to 0.6‰ from the $\delta^{13}C$ of seawater because of the formation of a phytodetritus layer at the sediment surface [*Mackensen et al.*, 1993]. This phenomenon, know as the "Mackensen phytodetritus effect," has been invoked as a possible explanation for the low $\delta^{13}C$ values exhibited by benthic foraminifera in the South Atlantic sector of the Southern Ocean during glacial intervals [*Mackensen et al.*, 2001]. Several South Atlantic sites do show evidence of increased surface water productivity coincident with the onset of Northern Hemisphere Glaciation at 2.75 Ma [*Sigman et al.*, 2004]. However, deep sea sediments in the region record a consistent glacial-interglacial shift in benthic $\delta^{13}C$, regardless of the productivity or sedimentary regime, which largely rules out the existence of a significant surface productivity overprint [*Ninnemann and Charles*,

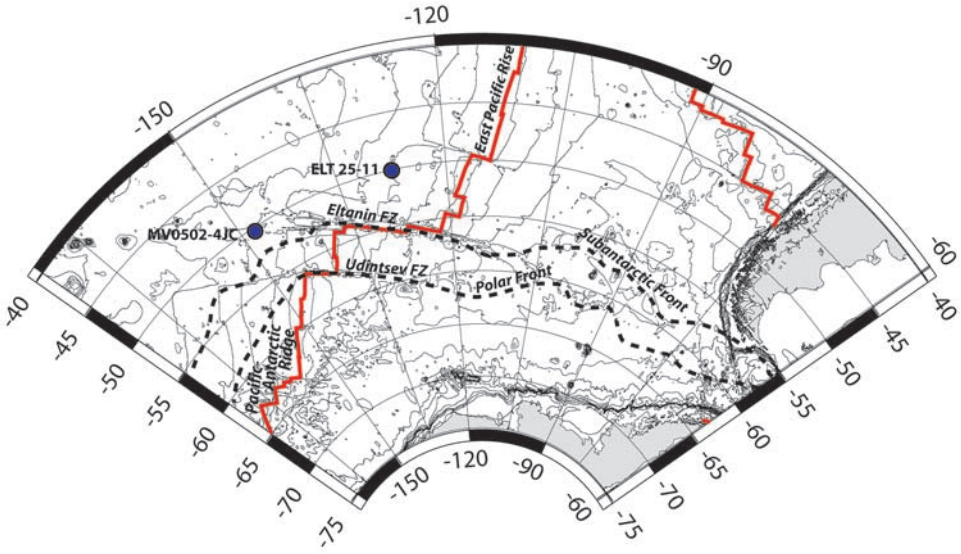

Figure 1. Bathymetric map of the study region, depicting the core locations of MV0502-4JC (50°20′S, 148°08′W, 4286 m) and ELT 25-11 (50°02′S, 127°31′W, 3969 m), for which new results are presented in this study. Red solid line represents the midocean ridge, and black dashed lines represent oceanic fronts. (Online Map Creation at www.aquarius.ifm-geomar.de.)

2002]. An alternative explanation is that the low $\delta^{13}C$ values reflect reduced ventilation of the deep Southern Ocean resulting from changes in the Antarctic source region during glacial intervals, such as increased sea ice cover, enhanced surface water stratification, decreased Ekman-induced upwelling, and reduced vertical mixing across the thermocline [*Hodell and Venz-Curtis*, 2006].

2.2. Setting and Oceanography

[12] Two carbonate-rich cores from the subantarctic Pacific region were examined in this study: MV0502-4JC (50°20′S, 148°08′W, 4286 m) and ELT 25-11 (50°02′S, 127°31′W, 3969 m) (Figure 1). These cores were recovered from the southern edge of the Southwest Pacific Basin near the Eltanin Fracture Zone system, a 1000 km offset between the Pacific Antarctic Ridge and the Southern East Pacific Rise [*Lonsdale*, 1994]. The Subantarctic Zone, which extends north from the Subantarctic Front to the Subtropical Front, is distinguished by the presence of Subantarctic Surface Water and biocalcareous sedimentation. An unusually deep carbonate compensation depth in the region of approximately 4750 m allows for the preservation of carbonate-rich sediments at abyssal depths [*Lyle et al.*, 2007]. To the south of the sites, the Subantarctic Front and the Polar Front are strongly guided by topography to flow though the Eltanin and Udintsev Fracture Zones [*Gille et al.*, 2004]. The close proximity of these fracture zones makes past migrations of the fronts over the sites unlikely.

[13] The deepwater mass bathing the core sites examined in this study is lower Circumpolar Deepwater (CDW). CDW, the deepwater mass of the Antarctic Circumpolar Current (ACC), is divided into three components, upper CDW (1400–2800 m), largely returning Pacific Deepwater (PDW) characterized by low oxygen and high nutrient concentrations, middle CDW (2800–3400 m), a high-salinity layer within the maximum influence of the NADW, and lower CDW (>3800 m), a cold, low-salinity water mass primarily composed of AABW [*Hall et al.*, 2003]. After AABW forms through the sinking of extremely cold shelf waters in regions such as the Weddell Sea, the Ross Sea, and the Adélie Coast, its flow is impeded by sills such as the Drake Passage, and because of its high density, AABW is largely confined to the Southern Ocean basins until entrained upward into the ACC. While AABW manages to enter the Atlantic Ocean through a deep gap in the South Scotia Ridge, AABW is thought to be ponded within the Australian-Antarctic and Southeast Pacific Basins by the ridge systems to the north [*Orsi et al.*, 1999]. Thus, the bottom water that ultimately fills the Southwest Pacific Basin, as well as the entire deep North Pacific, PDW, is water that has been sourced from the lower part of CDW and has been transported northward along the New Zealand platform by the Deep Western Boundary Current (DWBC), ultimately becoming warmer, fresher, oxygen-poorer, and nutrient-richer along its journey to the North Pacific [*Whitworth et al.*, 1999].

3. Methods

3.1. Processing and Analysis of the Sediment

[14] Sediment samples were washed with distilled water over a 63 μm sieve and oven-dried. Dry sediment samples were weighed both before and after and sieving in order to calculate the weight percent sediment >63 μm, Ice rafted debris and manganese micronodules were also counted from the >150 μm size range. For stable isotope analyses, foraminifera of similar size were picked from the >125 μm fraction, cleaned in methanol, and roasted under vacuum at 200°C for 1 h. Analyses were then conducted in the University of Michigan Stable Isotope Laboratory, where samples were

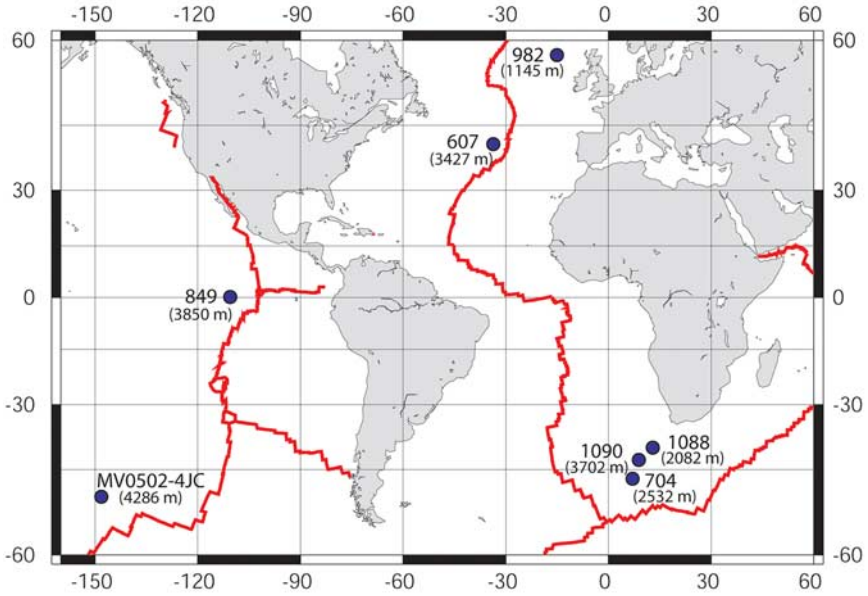

Figure 2. Map showing the location of existing benthic stable isotope records that are compared to MV0502-4JC in this study. Red solid line represents the midocean ridge. (Online Map Creation at www.aquarius.ifm-geomar.de.)

reacted at 75°C with phosphoric acid in a Kiel automatic carbonate preparation device linked to a Finnigan MAT 251 mass spectrometer. Stable isotope data are reported in standard δ notation relative to the Vienna Peedee belemnite (VPDB) standard. Analytical precision, which was monitored through the regular analysis of the standard reference carbonate NBS 19, was ±0.03‰ for δ^{13}C and ±0.08‰ for δ^{18}O (1σ, N = 153). Planktonic samples generally consisted of six specimens of *Globigerina bulloides*, and benthic samples consisted of three specimens of either *Cibicidoides mundulus* (*Cibicidoides kullenbergi*), *Planulina wuellerstorfi* (*Cibicidoides wuellerstorfi*), or *Cibicidoides robertsonianus*.

[15] A correction factor of +0.64‰ was applied to the benthic δ^{18}O values to correct for the known departures from isotopic equilibrium of *C. mundulus* and *P. wuellerstorfi* [*Shackleton and Hall*, 1997]. The same correction factor of +0.64‰ was also used for *C. robertsonianus* because comparison of the δ^{18}O values of *C. robertsonianus* and *P. wuellerstorfi* in samples containing specimens of both species demonstrated no significant offset. A correction factor was not applied to the benthic δ^{13}C values in this study because the δ^{13}C values of *C. mundulus* and *P. wuellerstorfi* are known to reflect equilibrium values [*Shackleton and Hall*, 1997]. The δ^{13}C value of *C. robertsonianus* also showed no significant offset from *P. wuellerstorfi* in multiple analyses carried out over the same sample interval.

3.2. Comparison to Existing Stable Isotope Records

[16] The benthic stable isotope record obtained from MV0502-4JC in this study is compared to existing late Neogene benthic stable isotope records from ODP Sites 607 and 982 in the North Atlantic, ODP Sites 704 and 1090 in the South Atlantic, and ODP Site 849 in the equatorial Pacific, as compiled by *Hodell and Venz-Curtis* [2006]. Pacific Site 849, located on the western flank of the East Pacific Rise, records the characteristics of average PDW from 0 to 9 Ma [*Mix et al.*, 1995]. Site 607, which is located on the western flank of the Mid Atlantic Ridge, monitors changes in lower NADW from 0 to 3.2 Ma [*Raymo et al.*, 1990], and Site 982 on the Rockall Plateau records the properties of upper NADW from 4.6 to 9.0 Ma [*Hodell et al.*, 2001]. The stable isotope records from Site 704 on the Meteor Rise and Site 1090/TN057-6 on the Agulhas Ridge [*Müller et al.*, 1991; *Hodell and Venz*, 1992; *Venz and Hodell*, 2002] were combined by *Hodell and Venz-Curtis* [2006] to create a single continuous record of CDW in the South Atlantic. Additionally, ODP Site 1088, also located on the Agulhaus Ridge, provides an important record of South Atlantic intermediate water (<2500 m) variation [*Billups*, 2002; *Hodell et al.*, 2003; *Hodell and Venz-Curtis*, 2006]. The locations of these sites are depicted in Figure 2, and the location and depth information for the stable isotope records discussed in this study can be found in Table 1.

4. Results

4.1. Chronology

4.1.1. MV0502-4JC

[17] A compilation of the results from MV0502-4JC (Figure 1; 50°20′S, 148°08′W, 4286 m) can be seen in Figure 3; raw data are provided in Data Sets S1 and S2.[1] The chronology was developed primarily on the basis of radiolarian and stable isotope stratigraphy (Table 2). To ensure that the core top was intact, ^{14}C analysis of *G. bulloides* was conducted at the University of Arizona AMS laboratory. Overall, MV0502-4JC was found to extend

[1]Auxiliary materials are available at ftp://ftp.agu.org/apend/pa/2008pa001661.

Table 1. Location and Water Depth of Late Neogene Stable Isotope Records Discussed in This Study

Site/Core	Location	Water Depth	References
ODP 704	46°52′S, 7°5′E	2532 m	*Hodell and Venz* [1992] and *Müller et al.* [1991]
ODP 1090	42°55′, 8°54′E	3702 m	*Venz and Hodell* [2002]
ODP 1088	41°08′S, 13°34′E	2082 m	*Billups* [2002], *Hodell et al.* [2003], and *Hodell and Venz-Curtis* [2006]
ODP 607	41°00′N, 33°37′W	3427 m	*Raymo et al.* [1990]
ODP 849	0°11′N, 110°31′W	3850 m	*Mix et al.* [1995]
ODP 982	57°31′N, 15°53′W	1145 m	*Hodell et al.* [2001]
MV0502-4JC	50°20′S, 148°08′W	4286 m	this study
ELT 25-11	50°02′S, 127°31′W	3969 m	this study

from the Holocene to the Late Miocene with three major hiatuses: an early Pliocene–early late Pliocene hiatus (hiatus A, between ~10.7 and 10.2 meters below seafloor (mbsf)), and two Pleistocene hiatuses from ~1.57–0.7 Ma (hiatus B, ~4 mbsf) and ~0.45–0.25 Ma (hiatus C, ~2.4 mbsf). Hiatus A was poorly constrained because of severe dissolution and reworking within the interval 10.7 to 10.2 mbsf.

[18] In the late Miocene portion of the core below hiatus C, an age model could not be constructed because of the presence of only one age datum, the late Miocene carbon shift (LMCS), a global event that has been dated to 7.7 to 6.6 Ma [*Tedford and Kelly*, 2004]. Radiolarians in the late Miocene portion of the core (~10.7 to 17.2 mbsf) yield age estimates of 10–13 Ma that are incongruous with the established timing of the LMCS (Table 2). The poor nature of the radiolarian record in this part of the core is likely a manifestation of an exceedingly low sedimentation rate and/or the lack of radiolarian species specific to this age range that would otherwise aid in the recognition of reworking. The LMCS, however, is easily identified by the permanent nature of the negative benthic δ^{13}C shift, a concurrent increase in carbonate dissolution, and the absence of an accompanying change in benthic δ^{18}O. In Figure 4, the carbon shift in MV0502-4JC has been aligned with that of Site 704 in order to facilitate comparison with other deep sea records.

[19] In the late Pliocene–early Pleistocene interval of the core between hiatuses A and B (~10.2–4 mbsf), an approximate age-depth relationship was developed to allow comparison with other deep-sea records (Figure 5). The most distinctive feature of this portion of the core is the late Pliocene climate transition (LPCT) [*Hodell and Ciesielski*, 1990; *Hodell and Venz*, 1992]. Because the sedimentation rate appears to increase within this interval, two separate linear age-depth models were used with a break at 7.32 mbsf, the depth at which we identify the MIS 71/72 boundary. Below 7.32 mbsf, we correlate the onset of the δ^{13}C shift with that of Site 704/1090 [*Hodell and Venz-Curtis*, 2006]. Above 7.32 mbsf, MIS 55–59 (1.585–1.698 Ma) were identified on the basis of their highly distinctive nature and a radiolarian age of 1.63–1.79 Ma at 5.12 mbsf. This allowed for the tentative assignment of MIS 61, 63, 67, and 71. These marine isotope stage assignments were then used to calculate a linear age-depth relation on the basis of the oxygen isotope stack of *Lisiecki and Raymo* [2005].

[20] The majority of the Pleistocene record after ~1.57 Ma was found to be missing because of hiatuses B and C, and the amplitudes of the few glacial-interglacial cycles represented below hiatus B (MIS 14–16 and MIS 2–6) have likely been reduced because of the low sedimentation rate. MIS 14–16 were identified on the basis of the distinctive nature of MIS 16 and a radiolarian age of 0.425–1.08 Ma at 2.57 mbsf, which distinguishes MIS 16 from MIS 12. Additionally, MIS 2–6 were constrained on the basis of radiocarbon dates taken from the top of the core and by the absence of *Stylatractus universus* (LO 0.425 Ma).

4.1.2. ELT 25-11

[21] In Figure 6, we present results from the Eltanin piston core ELT 25-11 (Figure 1; 50°02′S, 127°31′W, 3969 m), which was recovered approximately 1000 km to the east of MV0502-4JC on the flank of the East Pacific Rise; raw data are provided in Data Sets S3 and S4. The new radiolarian and stable isotope data acquired from ELT 25-11 have allowed for the improvement of an existing nannofossil chronology developed by *Geitzenauer and Huddlestun* [1972] and later modified by *King* [1988] (Table 3). Overall, the ELT 25-11 record extends into the late Pliocene, and the stable isotope record, while coarse, displays the distinctive late Pliocene features present in MV0502-4JC, including the positive benthic δ^{18}O and negative benthic δ^{13}C excursions of the LPCT and large positive planktonic and benthic δ^{13}C shifts of ~+1‰ near the late Pliocene/Pleistocene boundary. In the earlier chronology, a hiatus was placed at ~3.74 mbsf and assigned a maximum age range of ~1.95–0.30 Ma, but we suggest that the hiatus actually spans from 1.55 to 0.30 Ma and is located closer to 1.94 mbsf, synchronous with a significant drop in the $CaCO_3$ content. The original placement of the hiatus was based on the disappearance of *P. laconosa* above 3.89 mbsf. However, our radiolarian stratigraphy indicates an age of 1.73–1.85 Ma at 2.65 mbsf, and the large positive planktonic and benthic δ^{13}C shifts of ~1‰ that we identify in ELT 25-11 between ~3.24 and 2.54 mbsf clearly correlate to similar shifts that were dated to the early Pleistocene in MV0502-4JC.

4.2. Overview of the Results

4.2.1. Late Miocene

[22] Benthic δ^{18}O values between 17.17 and 12.11 mbsf are the lowest and least variable overall, averaging 3.59‰ (maximum, 3.85‰; minimum, 3.32‰) (Figure 3). Before the prominent negative benthic δ^{13}C shift of ~1‰ at ~15.3 mbsf, identified as the LMCS, δ^{13}C values average 1.13 ± 0.18‰. Following the shift, benthic δ^{13}C values average 0.28 ± 0.16‰. Benthic δ^{13}C values in MV0502-4JC are very similar to those recorded at Site 704 both before and after the LMCS, and benthic δ^{18}O values at the two sites are also comparable (Figure 4).

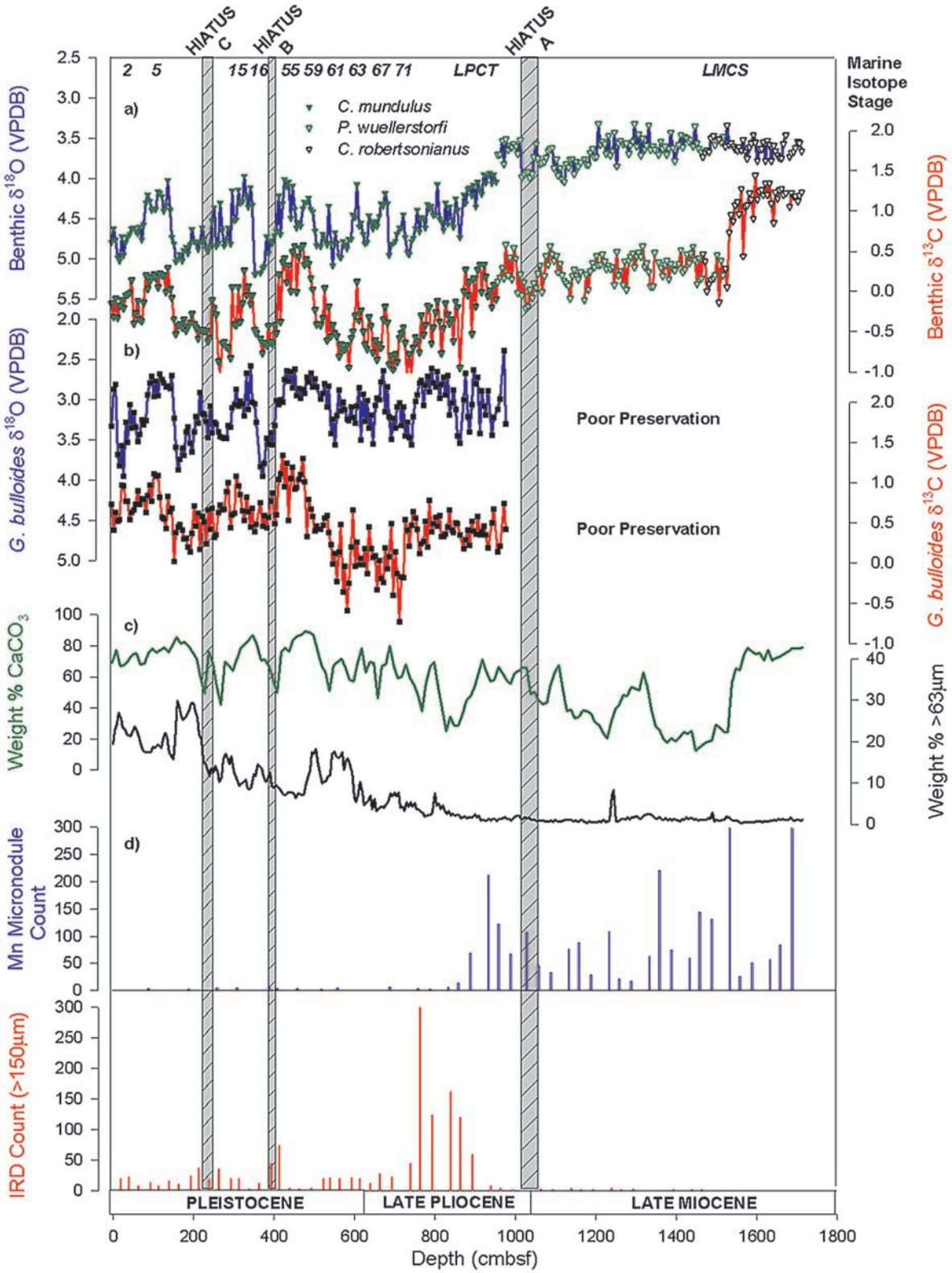
HIATUS C
HIATUS B
HIATUS A
2 5
15 16
55 59 61 63 67 71
LPCT
LMCS
Marine Isotope Stage
a)
C. mundulus
P. wuellerstorfi
C. robertsonianus
Benthic δ18O (VPDB)
Benthic δ13C (VPDB)
b)
G. bulloides δ18O (VPDB)
G. bulloides δ13C (VPDB)
Poor Preservation
Poor Preservation
c)
Weight % CaCO3
Weight % >63µm
d)
Mn Micronodule Count
IRD Count (>150µm)
PLEISTOCENE
LATE PLIOCENE
LATE MIOCENE
Depth (cmbsf)

Figure 3

Table 2. Important Age Datums Identified in MV0502-4JC

Depth (cm)	Age or Age Range	Basis for Age Assignment
	Radiocarbon Dates[a]	
4–6	9,849 ± 51	
16–18	16,799 ± 96	
	Radiolarian Biostratigraphy[b]	
166–168	<0.425	LO *Stylatractus universus*
256–258	0.425–1.08	LO *Stylatractus universus* and FO *Lamprocyrtis nigrinii*
391–393	1.08–1.63	FO *Lamprocyrtis nigrinii* and FO *Theocorythium trachelium*
511–513	1.63–1.79	FO *Theocorythium trachelium* and LO *Lamprocyrtis heteroporus*
806–808	1.85–2.38	FO *Triceraspyris antarctica* and FO *Antarctissa denticulata*
1021–1023	2.5–3.29	FO *Cycladophora davisiana* and FO *Lamprocyrtis heteroporus*
1071–1073[c]	10.1–11.89	LO *Carpocanopsis cristata* and LO *Cyrtocapsella tetrapera*
1141–1143[c]	11.89–11.94	LO *Cyrtocapsella tetrapera* and LO *Stauroxiphos communis*
1701–1703[c]	11.94–12.7	LO *Stauroxiphos communis* and FO *Antarctissa deflandrei*
	Stable Isotope Stratigraphy[b]	
1530	7.7–6.6	Late Miocene δ^{13}C shift [*Tedford and Kelly*, 2004]
962	~2.75	Late Pliocene δ^{13}C shift [*Hodell and Venz-Curtis*, 2006]
732	1.898	MIS 71/72 [*Lisiecki and Raymo*, 2005]
507	1.698	MIS 59/60 [*Lisiecki and Raymo*, 2005]
447	1.608	MIS 55/56 [*Lisiecki and Raymo*, 2005]
387	0.676	MIS 16/17 [*Lisiecki and Raymo*, 2005]
354.5	0.621	MIS 15/16 [*Lisiecki and Raymo*, 2005]
152	0.130	MIS 5/6 [*Lisiecki and Raymo*, 2005]
82	0.071	MIS 4/5 [*Lisiecki and Raymo*, 2005]

[a]Ages are in ka.
[b]Ages are in Ma.
[c]The radiolarians within this interval of the core are likely reworked.

[23] Sedimentation rates are very low throughout the late Miocene (≤0.25 cm/ka), and carbonate dissolution appears particularly severe following the LMCS (Figure 3). Before the LMCS, carbonate contents average ~70–80% and a few well-preserved planktonic foraminifera are present, although coccolithophorids account for most of the carbonate content. After the LCMS, weight percent carbonate falls to ~13–29% and whole planktonic foraminifera become exceedingly rare. Throughout the late Miocene, abundant manganese micronodules provide an additional indication of low sedimentation rates, and ice rafted debris is present only in trace amounts.

4.2.2. Late Pliocene

[24] Between 10.2 and 9.6 mbsf (~3.0–2.75 Ma), benthic δ^{18}O values average 3.63 ± 0.09‰ and are briefly comparable to late Miocene values (Figure 3). Benthic δ^{18}O resembles the Site 704 record, but benthic δ^{13}C values, which average 0.31 ± 0.17‰, are more Pacific-like than those at Site 704 (Figure 5). Between 9.6 and 7.3 mbsf (~2.75–1.9 Ma), MV0502-4JC displays dramatic changes associated with the late Pliocene climate transition (LPCT), most notably shifts in mean benthic δ^{18}O and δ^{13}C of ~+1.1‰ and ~−1.05‰, respectively. Following these shifts, δ^{18}O values are significantly higher than those recorded at Sites 704 and 1090. Overall, a comparison between the δ^{18}O values recorded by MV0502-4JC and those of deep equatorial Pacific Site 849, North Atlantic Site 607, and subantarctic Atlantic Sites 704/1090 suggests that mean δ^{18}O values were 0.75 to 1‰ higher at the site of MV0502-4JC (>4000 m water depth) than at the other sites toward the end of the late Pliocene (<2.4 Ma). Benthic δ^{13}C values are similar to those of deep equatorial Pacific Site 849 and subantarctic Atlantic Sites 704/1090 following the LPCT, but drift toward lower values by the end of the Pliocene.

[25] Following the benthic δ^{18}O and δ^{13}C shifts of the LPCT, ice rafted debris also becomes significant for the first time at ~8.9 mbsf and manganese micronodules decrease to trace amounts by ~8.4 mbsf (Figure 3). Initially, the benthic δ^{18}O and δ^{13}C shifts are associated with a decrease in the carbonate content between ~8.6 and 8.3 mbsf but are followed by an increase in the quality and quantity of planktonic foraminifera as well as an increase in the sedimentation rate to ~1.1 cm/ka by ~7.3 mbsf. Ash is present in samples throughout this interval and the reworking of radiolarians of Miocene-Oligocene age was noted at 8.07 mbsf.

[26] The record from ELT 25-11, while coarse, also shows significant shifts in benthic δ^{18}O and δ^{13}C during the LPCT (Figure 6). Benthic δ^{18}O shifts by ~+1.1‰ (from 3.6‰ to 4.7‰) between 6.3 and 3.7 mbsf, and benthic δ^{13}C shifts by ~−1.6‰ (from 1.09‰ to −0.5‰) over the same interval. While the δ^{18}O shift in ELT 25-11 is very similar to that of MV0502-4JC, the δ^{13}C shift is larger than that in MV0502-4JC because of significantly higher δ^{13}C values in ELT 25-11 preceding the LPCT.

4.2.3. Pleistocene

[27] Below hiatus B (~4.0 mbsf, ~1.57–0.68 Ma), a distinctive ~1‰ increase in the benthic and planktonic δ^{13}C values occurs between 5.62 and 4.77 mbsf (~1.7–1.65 Ma) (Figures 3 and 5). This ~1‰ increase in benthic and planktonic δ^{13}C is also recorded in ELT 25-11 between ~3.24 and 2.54 mbsf and marks the return of benthic δ^{13}C to values comparable to those recorded prior to the LPCT (Figure 6). Above hiatus B, carbonate contents recover and a strong, distinctive glacial event identified as MIS 16 occurs at ~3.77 mbsf (Figure 3). During MIS 16, both benthic and planktonic foraminifera exhibit the highest δ^{18}O values of the entire record, reaching maximum values of 5.19‰ and 3.95‰, respectively. Following MIS 15 and 14, hiatus C (~2.57 mbsf) is accompanied by two declines in $CaCO_3$ at 2.70 mbsf and 2.30 mbsf. Above hiatus C, we identify isotope

Figure 3. Compilation of the results from MV0502-4JC. (a) Benthic δ^{18}O represented by top line, and benthic δ^{13}C represented by bottom line. Solid green, open green, and open black triangles depict data points obtained from the benthic species *C. mundulus*, *P. wuellerstorfi*, and *C. robertsonianus*, respectively. (b) *G. bulloides* δ^{18}O represented by top line, and *G. bulloides* δ^{13}C represented by bottom line. (c) Weight percent $CaCO_3$ (top line) and weight percent of the sediment > 63 μm (bottom line). (d) Counts of manganese micronodules (top histogram) and ice rafted debris (bottom histogram) > 150 μm. Age constraints are from radiolarian and stable isotope stratigraphy. The ages assigned to the hiatuses are as follows: hiatus A, early Pliocene–early late Pliocene; hiatus B, ~1.57–0.68 Ma; and hiatus C, ~0.53–0.19 Ma.

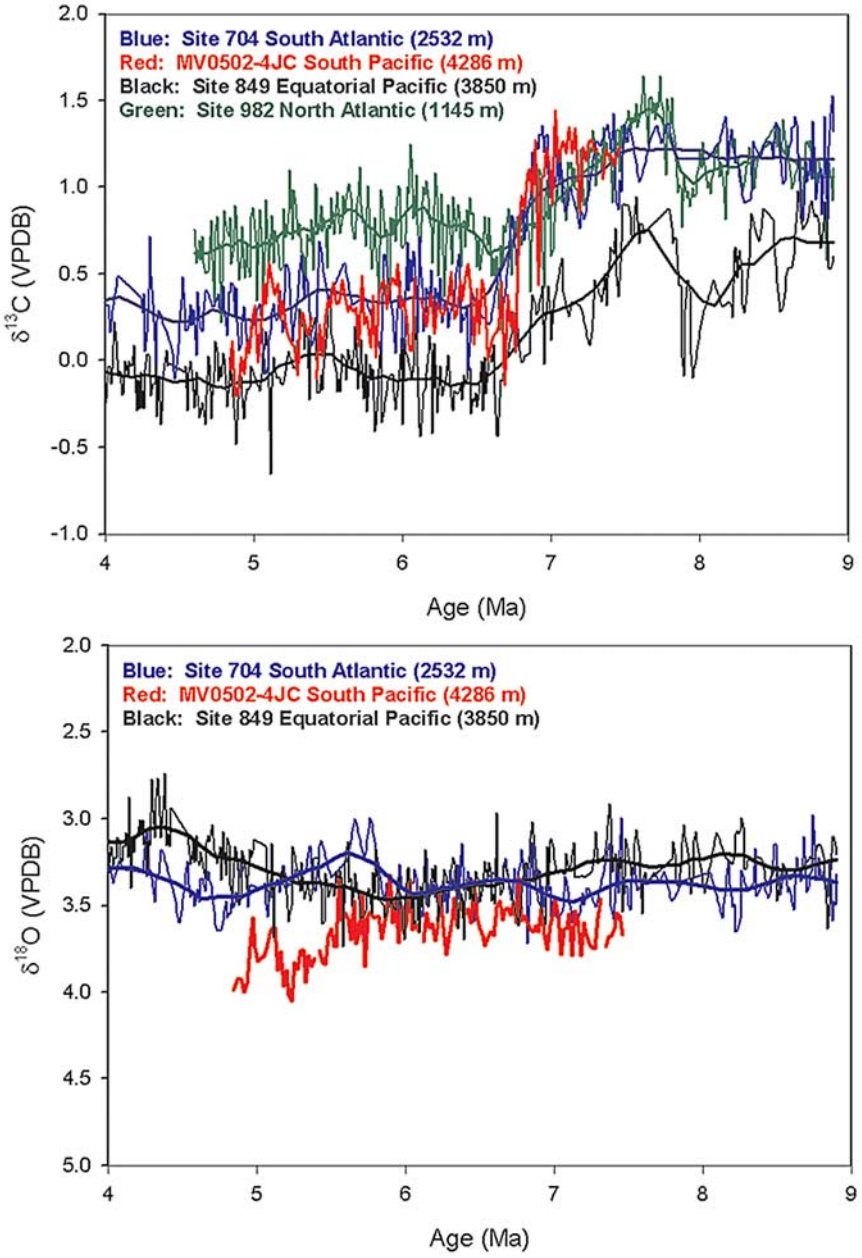

Figure 4. Comparison of the MV0502-4JC (red) (top) benthic δ^{13}C and (bottom) δ^{18}O records of the late Miocene carbon shift (LMCS) to ODP sites 849 (black, equatorial Pacific Ocean), 982 (green, North Atlantic), and 704 (blue, South Atlantic). The 25-point running mean of these records is also shown. However, the δ^{18}O record of Site 982 is not shown because of its shallow depth. Note that age constraints for MV0502-4JC in the late Miocene are limited to the LMCS, which we have aligned to the shift at Site 704.

stages 1–6. In this uppermost section of the core, the abundance of planktonic foraminifera reaches a maximum, and sedimentation rates are ~1.2 cm/ka.

5. Discussion

5.1. Late Miocene Carbon Shift

[28] The LMCS is a complicated and poorly understood event that may have consisted of at least two distinct components. First, the LMCS is likely linked to change in global carbon mass balance, as evidenced by the presence of a negative shift in the δ^{13}C records of both benthic and planktonic foraminifera [*Vincent et al.*, 1980]. The negative δ^{13}C shift could perhaps be explained by enhanced erosion and the addition of δ^{13}C-depleted organic soil material to the ocean under the expansion of C4 plants, a hypothesis not inconsistent with a spike in carbonate dissolution or the late Miocene biogenic bloom observed at many sites [*Diester-Haass et al.*, 2006]. *Cerling et al.* [1997] hypothesized that a drop in atmospheric CO_2 could have driven the expansion of

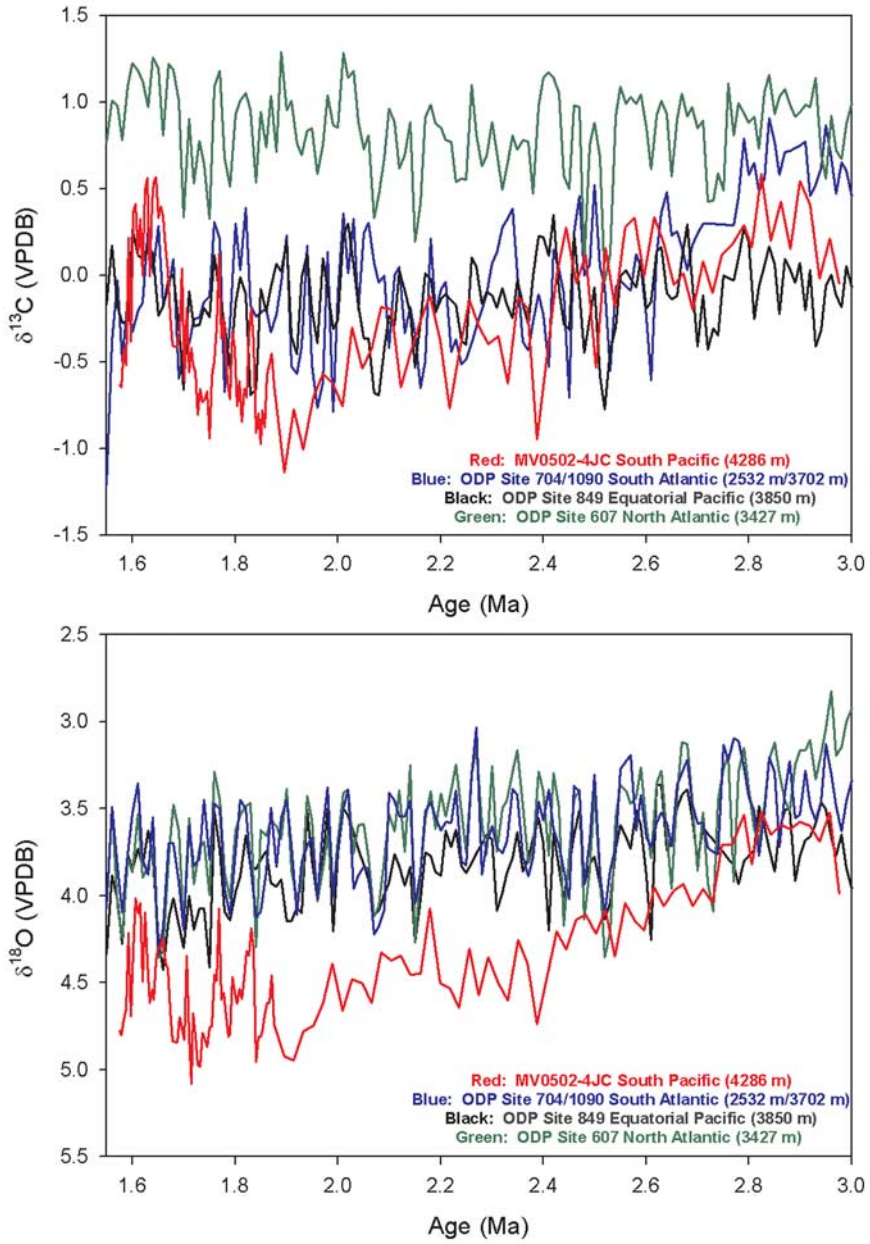

Figure 5. Comparison of the MV0502-4JC (red) (top) benthic $\delta^{13}C$ and (bottom) $\delta^{18}O$ records of the late Pliocene climate shift to records from ODP sites 849 (black, equatorial Pacific Ocean), 607 (green, North Atlantic), and 704/1090 (blue, South Atlantic).

C4 grasslands in the late Miocene because C4 photosynthesis is favored over the C3 pathway under low CO_2 conditions. This hypothesis has not been supported, however, by large differences in the timing of C4 expansion between continents [*Fox and Koch*, 2003], or by alkenone-based reconstructions of late Miocene atmospheric CO_2 levels [*Pagani et al.*, 1999].

[29] The transfer of carbon between the terrestrial and marine realms can offer only a partial explanation for the LMCS because the size of the $\delta^{13}C$ shift varies spatially. Thus, the LMCS likely also reflects a significant reorganization of interbasinal $\delta^{13}C$ gradients [*Vincent et al.*, 1980]. *Hodell and Venz-Curtis* [2006] emphasize the development of a modern interbasinal gradient between North Atlantic Site 982 and South Atlantic Sites 704 and 1088 during the LMCS. While benthic $\delta^{13}C$ values at Sites 704 and 982 were similar prior to the LMCS, the magnitude of the carbon shift was greater in the South Atlantic than the North Atlantic, thereby marking the inception of a modern interbasinal gradient in which South Atlantic $\delta^{13}C$ values fall about midway between those of the North Atlantic and Pacific (Figure 4).

[30] A longstanding explanation for the interbasinal $\delta^{13}C$ changes associated with the LMCS has been increased NADW production. NADW has a high ^{13}C content that

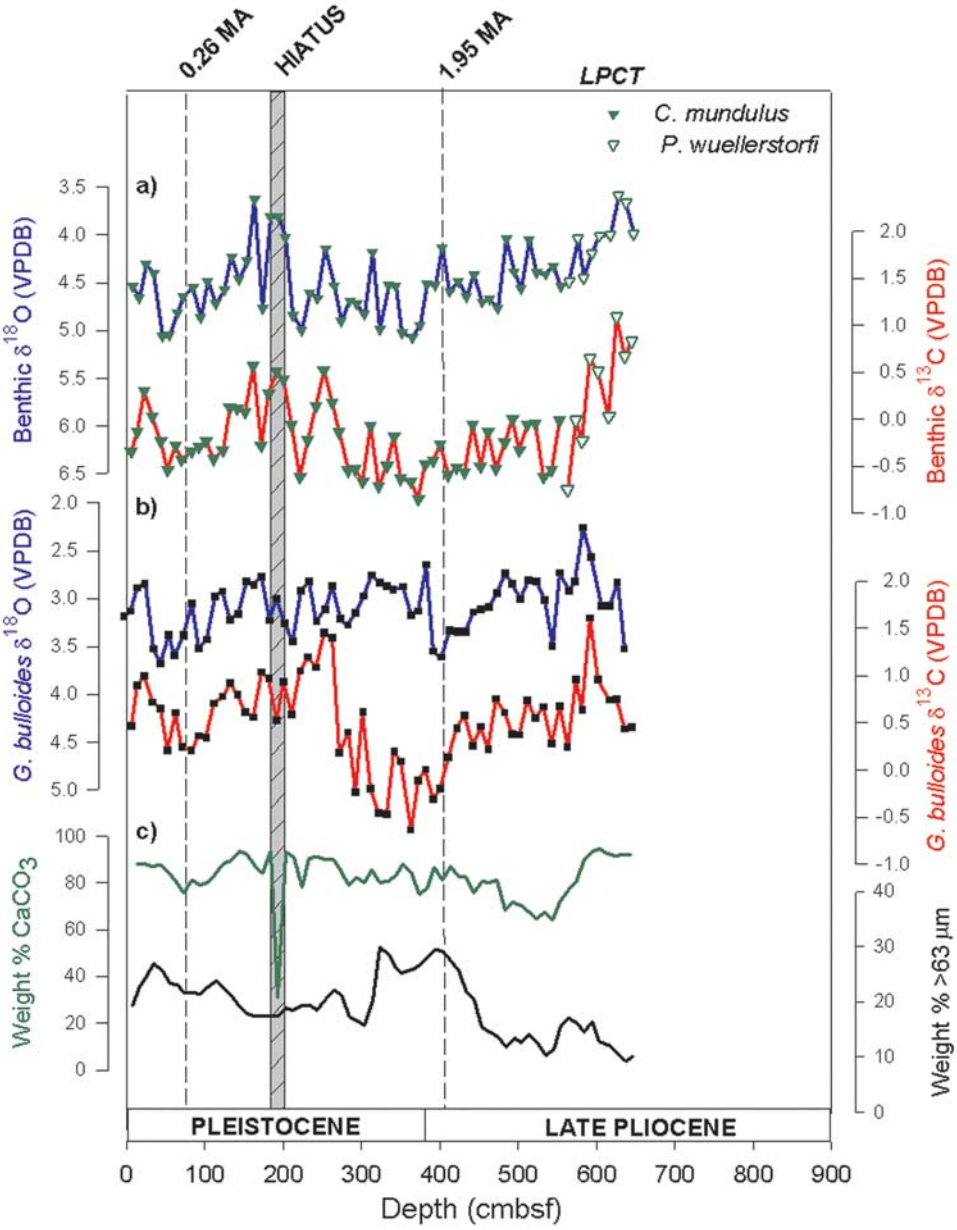

Figure 6. Compilation of the results from ELT 25-11. (a) Benthic δ^{18}O represented by top line and benthic δ^{13}C represented by bottom line. Solid green and open green triangles depict data points obtained from the benthic species *C. mundulus* and *P. wuellerstorfi*, respectively. (b) *G. bulloides* δ^{18}O represented by top line, and *G. bulloides* δ^{13}C represented by bottom line. (c) Weight percent $CaCO_3$ (top line) and weight percent of the sediment > 63 μm (bottom line). The age constraints shown (dashed lines) are from nannofossil biostratigraphy by *King* [1988]. The hiatus was assigned an age of ~1.55–0.3 Ma in this study.

would counteract an ocean-wide δ^{13}C decline within the North Atlantic region. Ocean-wide changes in carbonate preservation, including a deepening of the CCD [*Moore et al.*, 1984], suggest an increased presence of NADW in the Atlantic basin during the late Miocene. *Billups* [2002] argues on the basis of the carbon isotope record from Site 1088 that prior to 6.6 Ma, NADW did not extend into the Atlantic sector of the Southern Ocean and that after 6.6 Ma, tectonic changes, including the closure of the Central American Seaway or the subsidence of the Greenland-Scotland Ridge, led to an increased presence of NADW in the Atlantic basin. According to *Poore et al.* [2006], this increase in NADW strength occurred close to 6 Ma and was largely the result of subsidence of the Greenland-Scotland Ridge.

[31] An alternative explanation for the interbasinal δ^{13}C changes associated with the LMCS is a decrease in the preformed δ^{13}C value of AABW. Growth of the West

Table 3. Important Age Datums Identified in ELT 25-11

Depth (cm)	Age or Age Range (Ma)	Basis for Age Assignment
	Nannofossil Biostratigraphy	
74	0.26	CN14b/CN15 boundary [*King*, 1988]
404	1.95	CN12d/CN13a boundary [*King*, 1988]
	Radiolarian Biostratigraphy	
153–154	<0.425	LO *Stylatractus universus*
264–266	1.73–1.85	LO *Cycladophora pliocenica* and FO *Triceraspyris antarctica*
334–336	1.73–1.85	LO *Cycladophora pliocenica* and FO *Triceraspyris antarctica*
	Stable Isotope Stratigraphy	
647	~2.75	Late Pliocene δ^{13}C shift [*Hodell and Venz-Curtis*, 2006]

Antarctic Ice Sheet (WAIS) has been widely assigned to late Miocene [*Ciesielski et al.*, 1982; *Kennett and Barker*, 1990] (although most open marine records show no corroborating increase in benthic δ^{18}O), and establishment of the WAIS may have marked the initiation of bottom water formation processes in the Southern Ocean similar to those of the modern day (i.e., under ice shelves) [*Hodell and Venz-Curtis*, 2006]. Assuming the transfer of carbon from the terrestrial to the oceanic reservoir during the LMCS, a decrease in the preformed δ^{13}C signature of AABW would have acted to augment a decline in deepwater δ^{13}C values in the Southern and Pacific Oceans while having little effect on δ^{13}C values in the North Atlantic.

[32] Interestingly, we find in this study that benthic δ^{13}C values at the site of MV0502-4JC were similar to those of Site 704 both before and after the LMCS (Figure 4). Thus, the results from MV0502-4JC agree with the interpretation of *Hodell and Venz-Curtis* [2006] that the LMCS marked the development of modern-like δ^{13}C gradients between the North Atlantic, Pacific, and Southern Oceans. More importantly, however, these results show that the Southern Ocean remained well mixed following the LMCS, comparable to the present-day state in which it exhibits a relatively uniform δ^{13}C value of ~0.4‰. Expansion of the WAIS may have forced a decrease in the preformed δ^{13}C value of AABW during the LMCS, but this expansion was not accompanied by the initiation of a significant horizontal or vertical δ^{13}C gradient within the Southern Ocean. The formation of a chemocline in the Southern Ocean at ~2500 m would thus accompany a later stage of climatic cooling.

[33] It is important to emphasize that while the benthic δ^{13}C records from MV0502-4JC and ODP Sites 982, 704, 1088, and 849 are consistent with an increase in the supply of carbon to the oceans as well as the evolution of a modern interbasinal δ^{13}C gradient between the North Atlantic, Pacific, and Southern Oceans during the LMCS, other marine records do present a more complicated picture of the late Miocene ocean. In particular, following the LMCS benthic δ^{13}C values at ODP Site 1172 (43°57.57′S, 149°55.70′E, 2620 m) on the East Tasman Plateau stabilize at ~0.5–0.8‰ [*Tedford and Kelly*, 2004], lower than δ^{13}C values recorded at North Atlantic ODP Site 982 but higher than those recorded in the subantarctic region (ODP Site 704 and MV0502-4JC). Also, *Grant and Dickens* [2002] report an ~2 million year temporal offset between the negative δ^{13}C shift in planktonic foraminifera and bulk carbonate at DSDP Site 590 in the Tasman Sea, challenging the notion that the δ^{13}C decrease was a globally synchronous datum in all phases of biogenic carbonate. *Grant and Dickens* [2002] attribute this lag to changes in thermocline structure and nutrient cycling during the LMCS, although a change in the coccolithophorid species assemblage could offer an alternative explanation.

5.2. Late Pliocene Climate Transition

[34] Unlike the LMCS, which brought subtle changes to the Southern Ocean, the LPCT marked the onset of a dramatic shift within the abyssal Southern Ocean, particularly at the site of MV0502-4JC. In general, the LPCT is known for a series of δ^{18}O enrichment events of increasing magnitude at 3.1, 2.7, 2.6, and 2.4 Ma that signal the onset and gradual amplification of Northern Hemisphere Glaciation [*Keigwin*, 1986]. The magnitude of these late Pliocene glacial-interglacial δ^{18}O variations is not particularly impressive when compared to the climatic oscillations of the late Pleistocene. At Site 607, for example, δ^{18}O values oscillate 0.5‰ between 3.1 and 2.95 Ma and 0.9‰ between 2.7 and 2.4 Ma, compared to 1.75‰ during the last glaciation, and it was not until after 2.95 Ma that "glacial" δ^{18}O values at Site 607 became more positive than those of the present interglacial [*Raymo et al.*, 1992]. Thus, on the basis of the relatively small amplitude of late Pliocene glacial-interglacial δ^{18}O variations alone, the LPCT has not generally been regarded as a period dramatic oceanic change. However, following the first ODP cruise to the subantarctic Atlantic, *Hodell and Ciesielski* [1990] discovered that Site 704 recorded an interesting feature during the LPCT that deep sea cores from other regions did not: a 0.5‰ decrease in mean benthic δ^{13}C.

[35] Prior to the LPCT, δ^{13}C values at Site 704 had increased to once again become very similar to those of the North Atlantic, and thus the interbasinal gradient that had developed between the North and South Atlantic during to the LMCS had lessened significantly [*Hodell and Venz-Curtis*, 2006]. However, after ~2.75 Ma, δ^{13}C values at Site 704 underwent a sharp decline [*Hodell and Venz*, 1992; *Hodell et al.*, 2002]. *Hodell and Venz* [1992] explained the decrease in δ^{13}C in the South Atlantic as a decline in NADW formation after 2.7 Ma. In support of this interpretation, data from equatorial Atlantic ODP Sites 925 and 929 reveal that the NADW/AABW boundary in the Atlantic was at reduced depth during the late Pliocene (~2.6–2.1 Ma), suggesting a greater influence of southern source water during that period. However, *Hodell and Venz-Curtis* [2006] also noticed that while mean benthic δ^{13}C values at Site 704 declined during the LPCT, δ^{13}C values at Site 1088 remained the same, marking the development of a chemical divide in the South Atlantic basin at ~2500 m depth. Thus, the δ^{13}C shift recorded at Site 704 appears to be the reflection of not only a decline in NADW during the LPCT, but also a significant reduction in the ventilation of the deep Southern Ocean, as first proposed by *Hodell and Ciesielski* [1990].

[36] *Hodell and Venz-Curtis* [2006] suggest that increased sea ice and enhanced surface water stratification impeded air-sea gas exchange and contributed to lower preformed δ^{13}C

values in AABW during glacial periods after 2.75 Ma. The LPCT definitely brought significant changes to the Antarctic cryosphere, including the first significant ice rafting to MV0502-4JC and Sites 704 and 1092 [*Warnke et al.*, 1992; *Murphy et al.*, 2002], the development of a strong halocline at 2.73 Ma [*Haug et al.*, 1999; *Sigman et al.*, 2004], and significant sea ice expansion by ~2.5–2.4 Ma [*Burckle et al.*, 1990; *Kennett and Barker*, 1990]. Moreover, because these changes coincide with the onset of Northern Hemisphere Glaciation, the Southern Ocean has been suggested as a possible player in the growth of the Northern Hemisphere ice sheets [*Hodell and Ciesielski*, 1990; *Sigman et al.*, 2004; *Hodell and Venz-Curtis*, 2006]. As discussed below, the new stable isotope records from MV0502-4JC and ELT 25-11 lend additional weight to this idea.

[37] Like Site 704, the benthic stable isotope records from MV0502-4JC and ELT 25-11 also record a significant decline in δ^{13}C around the LPCT. However, while the LPCT at Site 704 appears to record the onset of a glacial-interglacial pattern of deep water ventilation in the Southern Ocean, with consistently poorer ventilation during glacials than interglacials, combined with a significant episode of δ^{18}O enrichment, the transition in MV0502-4JC and ELT 25-11 appears to signal a far more dramatic shift in conditions in the abyssal Southern Ocean. First, the benthic δ^{13}C shift is more extensive and prolonged in these deep subantarctic Pacific records than in the preexisting records from the South Atlantic, and second, the δ^{13}C decrease was matched by an equally dramatic increase in benthic δ^{18}O that stands out among other deep sea records from that period. Particularly unusual is the length of time that the low δ^{13}C values, and hence poorly ventilated conditions, persisted in MV0502-4JC and ELT 25-11, as well as the dramatic return of the δ^{13}C values to pre-LPCT values after ~1.7 Ma, which is recorded as a 1‰ increase in both the benthic and planktonic records.

[38] We interpret these benthic δ^{13}C and δ^{18}O shifts, which in MV0502-4JC amount to −1.05‰ and +1.1‰, respectively, over the period 2.7 to 1.9 Ma (9.6–7.3 mbsf), as an indication that the abyssal Southern Ocean was filled with very cold, poorly ventilated waters following the LPCT. Whereas we have found that benthic δ^{18}O values > 4.5‰ were attained in the abyssal (>4000 m water depth) subantarctic Pacific during the latest Pliocene, δ^{18}O values that high were not recorded at Sites 607, 849, and 704 until the glaciations of the late Pleistocene, at which time the temperature of the deep Atlantic, Pacific, and Southern Oceans is thought to have been within error of freezing point of seawater [*Adkins et al.*, 2002]. The cold, salty bottom waters that filled the deep ocean during the LGM were likely supplied through increased brine rejection [*Adkins et al.*, 2002], and sea ice expansion may have had a similar effect on the deepest waters of the Southern Ocean during the late Pliocene. Further support for a dramatic cooling of Antarctic bottom waters during the LPCT comes from the results of *Hayward et al.* [2007], who found that a succession of pulsed declines and extinctions of benthic foraminifera with unusual aperture types originated in southern sourced deep waters (AABW and CDW) during the late Pliocene, later extending into NADW and Antarctic Intermediate Water (AAIW) during the mid-Pleistocene climate transition (MPT, 1.2–0.55 Ma). Thus, by 2.4 Ma, as the Northern Hemisphere was beginning to grow ice sheets and the magnitude of the benthic δ^{18}O oscillations was just more than half that of the last glacial-interglacial cycle, it appears that sea ice expansion around Antarctica may have forced the abyssal Southern Ocean into a state not significantly unlike that of the LGM.

[39] These new stable isotope records from the abyssal subantarctic Pacific call for further examination of the role of the Southern Ocean in the LPCT. The progressive nature of the δ^{18}O and δ^{13}C shifts between 2.7 and 1.9 Ma suggests that an ever larger percentage of cold, poorly ventilated AABW accumulated in the abyssal Southern Ocean over this period as a result of increasingly pervasive sea ice cover. Intense sea ice formation would have increased the density of the deepest waters in the Southern Ocean and likely would have decreased the upwelling of these waters, allowing for the buildup of biologically fixed carbon in the abyssal Southern Ocean [*Watson and Naveira Garabato*, 2006]. Because the core sites of MV0502-4JC and ELT 25-11 are located just outside of the Southern Ocean basin, and thus record the signature of lower CDW rather than AABW itself, we infer that, at a minimum, the pool of cold, poorly ventilated water was sizable enough to fill the Pacific sector of the Southern Ocean below a depth of 4000 m. The existence of such a large, isolated water mass in the abyssal Southern Ocean during the late Pliocene is not only a surprising finding but also has significant implications for the amplification of Northern Hemisphere Glaciation during that period.

[40] This pool of poorly ventilated water appears to have persisted until 1.7 Ma, at which time the δ^{13}C values in MV0502-4JC and ELT 25-11 show a return to pre-LPCT values and the initiation of a more "typical" pattern of glacial-interglacial variation. Planktonic δ^{13}C values, which were also unusually low during the latest Pliocene and earliest Pleistocene, also increase at 1.7 Ma. This increase in benthic and planktonic δ^{13}C is consistent with global δ^{13}C maximum IV (MIS 53–57) identified by *Wang et al.* [2004] in several deep sea records. Other δ^{13}C maxima occur at MIS 13 and MIS 27–29 and precede the significant climatic transitions of the mid-Brunhes event and the mid-Pleistocene revolution [*Wang et al.*, 2004]. These δ^{13}C maxima have been associated with profound reorganizations of the global carbon reservoir and have been linked to changes in productivity, the oceanic "rain ratio," and increased carbonate dissolution in the Indo-Pacific [*Wang et al.*, 2004]. Thus, the increase in benthic δ^{13}C in MV0502-4JC and ELT 25-11 after 1.7 Ma likely reflects in part a whole-ocean shift in the δ^{13}C of DIC, but the shift is unusually large relative to the other deep sea sites examined in this study and thus raises the question of whether these cores might also record the first significant trend toward well-mixed, well-ventilated conditions in the abyssal Southern Ocean following the LPCT.

6. Conclusion

[41] The new abyssal subantarctic Pacific stable isotope record from MV0502-4JC presented in this study supports the finding of *Hodell and Venz-Curtis* [2006] that the LMCS

marked an important step in the evolution of the modern $\delta^{13}C$ gradient between the North Atlantic, Pacific, and Southern Ocean basins. While benthic $\delta^{13}C$ values at South Atlantic Site 704 and North Atlantic Site 982 were similar prior to the LMCS, the magnitude of the carbon shift was greater in the South Atlantic than the North Atlantic, thus marking the inception of the modern interbasinal $\delta^{13}C$ gradient in which South Atlantic $\delta^{13}C$ values fall midway between those of the North Atlantic and Pacific. New results from MV0502-4JC indicate that benthic $\delta^{13}C$ and $\delta^{18}O$ values in the abyssal subantarctic Pacific were nearly identical to those at South Atlantic Site 704 both before and after the LMCS. Thus, the South Atlantic and South Pacific sectors of the Southern Ocean responded similarly to the LMCS, and despite potential cryospheric changes, the LMCS did not mark the initiation of any interbasinal or vertical stable isotope gradients within the Southern Ocean. Instead, communication between the Atlantic and Pacific sectors of the Southern Ocean remained strong, and the water column appears to have been well mixed and homogenous during the late Miocene, similar to the Southern Ocean today.

[42] The late Pliocene climate transition (LPCT), in sharp contrast to the LMCS, did mark the development of significant vertical $\delta^{13}C$ and $\delta^{18}O$ gradients in the deep Southern Ocean. From the results of *Hodell and Ciesielski* [1990] and *Hodell and Venz-Curtis* [2006], we know that $\delta^{13}C$ values at Site 704 declined by 0.5‰ at 2.7 Ma while $\delta^{13}C$ values at intermediate Site 1088 remained unchanged, marking the development of a chemical divide in the South Atlantic basin at ~2500 m depth. However, the results of our study of the abyssal subantarctic Pacific cores MV0502-4JC and ELT 25-11 reveals that the abyssal Southern Ocean experienced changes during the LPCT that were far greater than those at Site 704. MV0502-4JC records benthic $\delta^{13}C$ and $\delta^{18}O$ shifts of −1.05‰ and +1.1‰, respectively, over the period 2.7 to 1.9 Ma (9.6–7.3 mbsf), which indicates that the abyssal Southern Ocean was filled with very cold, poorly ventilated waters consistent with extensive sea ice expansion during the late Pliocene [*Burckle et al.*, 1990; *Kennett and Barker*, 1990]. Increased sea ice cover and enhanced surface water stratification likely reduced air-sea gas exchange and contributed to lower preformed $\delta^{13}C$ values in AABW after ~2.7 Ma [*Hodell and Venz-Curtis*, 2006], but the low $\delta^{13}C$ values recorded in the abyssal subantarctic Pacific may also reflect the accumulation of respired CO_2 in the abyssal ocean as these cold, salty bottom waters resisted upwelling [*Watson and Naveira Garabato*, 2006]. The sea ice and the cold, poorly ventilated bottom waters appear to have persisted in the Southern Ocean until ~1.7 Ma at which time the reventilation of the Southern Ocean is recorded in both the benthic and planktonic $\delta^{13}C$ records as an increase of ~+1‰. Thus, while this study cannot identify the cause of the LPCT itself, we have found that the LPCT led to the development of an isolated, poorly ventilated water mass in the abyssal Southern Ocean, the existence of which may have important implications for the expansion of the Northern Hemisphere ice sheets in the late Pliocene.

[43] **Acknowledgments.** The South Pacific latitudinal transect cruise was supported by the National Science Foundation grants OCE-0240924 to University of Michigan and OCE–0240906 to Boise State University. We wish to thank David Hodell; an anonymous reviewer; and the editor, Gerald Dickens, for thoughtful comments that helped to improve this manuscript and Lora Wingate of the University of Michigan Stable Isotope Laboratory for the carbonate analyses. L. M. Waddell was supported through grants from Rackham Graduate School and the Sweetland Dissertation Writing Institute during the preparation of this manuscript.

References

Adkins, J. F., K. McIntyre, and D. P. Schrag (2002), The salinity, temperature, and $\delta^{18}O$ of the glacial deep ocean, *Science*, *298*, 1769–1773, doi:10.1126/science.1076252.

Billups, K. (2002), Late Miocene through early Pliocene deep water circulation and climate change viewed from the sub-Antarctic South Atlantic, *Palaeogeogr. Palaeoclimatol. Palaeoecol.*, *185*, 287–307, doi:10.1016/S0031-0182(02)00340-1.

Broecker, W. S., and E. Maier-Reimer (1992), The influence of air and sea exchange on the carbon isotope distribution in the sea, *Global Biogeochem. Cycles*, *6*, 315–320, doi:10.1029/92GB01672.

Brunelle, B. G., D. M. Sigman, M. S. Cook, L. D. Keigwin, G. H. Haug, B. Plessen, G. Schettler, and S. L. Jaccard (2007), Evidence from diatom-bound nitrogen isotopes for subarctic Pacific stratification during the last ice age and a link to North Pacific denitrification changes, *Paleoceanography*, *22*, PA1215, doi:10.1029/2005PA001205.

Burckle, L. H., R. Gersonde, and N. Abrams (1990), Late Pliocene-Pleistocene paleoclimate in the Jane Basin region: ODP Site 697, *Proc. Ocean Drill. Program Sci. Results*, *113*, 803–809.

Cerling, T. E., J. M. Harris, B. J. MacFadden, M. G. Leakey, J. Quade, V. Eisenmann, and J. R. Ehleringer (1997), Global vegetation change through the Miocene/Pliocene boundary, *Nature*, *389*, 153–158, doi:10.1038/38229.

Charles, C. D., and R. G. Fairbanks (1990), Glacial and interglacial changes in the isotopic gradients of Southern Ocean surface water, in *Geological History of the Polar Oceans: Arctic Versus Antarctic*, edited by U. Bleil and J. Theide, pp. 519–538, Kluwer Acad., Norwell, Mass.

Ciesielski, P. F., M. T. Ledbetter, and B. B. Ellwood (1982), The development of Antarctic glaciation and the Neogene paleoenvironment of the Maurice Ewing Bank, *Mar. Geol.*, *46*, 1–51, doi:10.1016/0025-3227(82)90150-5.

de Boer, A. M., D. M. Sigman, J. R. Toggweiler, and J. L. Russell (2007), Effect of global ocean temperature change on deep ocean ventilation, *Paleoceanography*, *22*, PA2210, doi:10.1029/2005PA001242.

Diester-Haass, L., K. Billups, and K. C. Emeis (2006), Late Miocene carbon isotope records and marine biological productivity: Was there a (dusty) link?, *Paleoceanography*, *21*, PA4216, doi:10.1029/2006PA001267.

Fox, D. L., and P. L. Koch (2003), Tertiary history of C_4 biomass in the Great Plains, USA, *Geology*, *31*, 809–812, doi:10.1130/G19580.1.

Francois, R., M. A. Altabet, E.-F. Yu, D. M. Sigman, M. P. Bacon, M. Frank, G. Bohrmann, G. Bareille, and L. D. Labeyrie (1997), Contribution of Southern Ocean surface-water stratification to low atmospheric CO_2 concentrations during the last glacial period, *Nature*, *389*, 929–935, doi:10.1038/40073.

Geitzenauer, K. R., and P. Huddlestun (1972), An upper Pliocene-Pleistocene calcareous nannofossil flora from a subantarctic Pacific deep-sea core, *Micropaleontology*, *18*, 405–409, doi:10.2307/1485048.

Gille, S. T., E. J. Metzger, and R. Tokmakian (2004), Seafloor topography and ocean circulation, *Oceanography*, *17*(1), 47–54.

Grant, K. M., and G. R. Dickens (2002), Coupled productivity and carbon isotope records in the southwest Pacific Ocean during the late Miocene–early Pliocene biogenic bloom, *Palaeogeogr. Palaeoclimatol. Palaeoecol.*, *187*, 61–82, doi:10.1016/S0031-0182(02)00508-4.

Hall, I. R., I. N. McCave, R. Zahn, L. Carter, P. C. Knutz, and G. P. Weedon (2003), Paleocurrent reconstruction of the deep Pacific inflow during the middle Miocene: Reflections of East Antarctic Ice Sheet growth, *Paleoceanography*, *18*(2), 1040, doi:10.1029/2002PA000817.

Haq, B. U., T. R. Worsley, L. H. Burckle, R. G. Douglas, L. D. Keigwin Jr., N. D. Opdyke, S. M. Savin, M. A. Sommer II, E. Vincent, and F. Woodruff (1980), Late Miocene marine

carbon-isotopic shift and synchroneity of some phytoplanktonic biostratigraphic events, *Geology*, *8*, 427–431, doi:10.1130/0091-7613(1980)8<427:LMMCSA>2.0.CO;2.

Haug, G. H., D. M. Sigman, R. Tiedemann, T. F. Pederson, and M. Sarnthein (1999), Onset of permanent stratification in the subarctic Pacific Ocean, *Nature*, *401*, 779–782, doi:10.1038/44550.

Hayward, B. W., S. Kawagata, H. R. Grenfell, A. T. Sabaa, and T. O'Neill (2007), Last global extinction in the deep sea during the mid-Pleistocene climate transition, *Paleoceanography*, *22*, PA3103, doi:10.1029/2007PA001424.

Hodell, D. A., and P. F. Ciesielski (1990), Southern Ocean response to the intensification of Northern Hemisphere glaciation at 2.4 Ma, in *Geological History of the Polar Oceans: Arctic Versus Antarctic*, edited by U. Bleil and J. Theide, pp. 707–728, Kluwer Acad., Dordrecht, Netherlands.

Hodell, D. A., and K. Venz (1992), Toward a high-resolution stable isotope record of the Southern Ocean during the Pliocene-Pleistocene (4.8 to 0.8 Ma), in *The Antarctic Paleoenvironment: A Perspective on Global Change, Part One*, *Antarct. Res. Ser.*, vol. 56, edited by J. P. Kennett and D. A. Warnke, pp. 265–310, AGU, Washington, D. C.

Hodell, D. A., and K. A. Venz-Curtis (2006), Late Neogene history of deepwater ventilation in the Southern Ocean, *Geochem. Geophys. Geosyst.*, *7*, Q09001, doi:10.1029/2005GC001211.

Hodell, D. A., J. H. Curtis, F. J. Sierro, and M. E. Raymo (2001), Correlation of late Miocene to early Pliocene sequences between the Mediterranean and North Atlantic, *Paleoceanography*, *16*(2), 164–178, doi:10.1029/1999PA000487.

Hodell, D. A., R. Gersonde, and P. Blum (2002), Leg 177 synthesis: Insights into Southern Ocean paleoceanography on tectonic to millennial timescales, *Proc. Ocean Drill. Program Sci. Results*, *177*, 1–54.

Hodell, D. A., K. A. Venz, C. D. Charles, and U. S. Ninnemann (2003), Pleistocene vertical carbon isotope and carbonate gradients in the South Atlantic sector of the Southern Ocean, *Geochem. Geophys. Geosyst.*, *4*(1), 1004, doi:10.1029/2002GC000367.

Jaccard, S. L., G. H. Haug, D. M. Sigman, T. F. Pederson, H. R. Thierstein, and U. Röhl (2005), Glacial/interglacial changes in subarctic North Pacific stratification, *Nature*, *308*, 1003–1006.

Keigwin, L. D. (1986), Pliocene stable-isotope record of Deep Sea Drilling Project Site 606: Sequential events of ^{18}O enrichment beginning at 3.1 Ma, *Initial Rep. Deep Sea Drill. Proj.*, *94*, 911–920.

Kennett, J. P., and P. F. Barker (1990), Latest Cretaceous to Cenozoic climate and oceanographic developments in the Weddell Sea, Antarctica: An ocean-drilling perspective, *Proc. Ocean Drill. Program Sci. Results*, *113*, 937–960.

King, R. E. Jr. (1988), *Sediment Distribution, Accumulation Rates, and Climatic Change in the Southeast Pacific*, 179 pp., Univ. of South. Miss., Hattiesburg, Miss.

Kohfeld, K. E., C. Le Quéré, S. P. Harrison, and R. F. Anderson (2005), Role of marine biology in glacial-interglacial CO_2 cycles, *Science*, *308*, 74–78, doi:10.1126/science.1105375.

Kroopnick, P. M. (1985), The distribution of ^{13}C of ΣCO_2 in the world oceans, *Deep Sea Res., Part A*, *32*, 57–84, doi:10.1016/0198-0149(85)90017-2.

Lisiecki, L. E., and M. E. Raymo (2005), A Pliocene-Pleistocene stack of 57 globally distributed benthic $\delta^{18}O$ records, *Paleoceanography*, *20*, PA1003, doi:10.1029/2004PA001071.

Lonsdale, P. (1994), Structural geomorphology of the Eltanin fault system and adjacent transform faults of the Pacific-Antarctic plate boundary, *Mar. Geophys. Res.*, *16*, 105–143, doi:10.1007/BF01224756.

Lunt, D. J., G. L. Foster, A. M. Haywood, and E. J. Stone (2008), Late Pliocene Greenland glaciation controlled by a decline in atmospheric CO_2 levels, *Nature*, *454*, 1102–1106, doi:10.1038/nature07223.

Lyle, M., S. Gibbs, T. C. Moore, and D. K. Rea (2007), Late Oligocene initiation of the Antarctic Circumpolar Current: Evidence from the South Pacific, *Geology*, *35*, 691–694, doi:10.1130/G23806A.1.

Lynch-Stieglitz, J., T. F. Stocker, W. S. Broecker, and R. G. Fairbanks (1995), The influence of air-sea exchange on the isotopic composition of oceanic carbon: Observations and modeling, *Global Biogeochem. Cycles*, *9*, 653–665, doi:10.1029/95GB02574.

Mackensen, A., H.-W. Hubberten, T. Bickert, G. Fischer, and D. K. Fütterer (1993), The $\delta^{13}C$ in benthic foraminiferal tests of *Fantbotia wuellerstorfi* (Schwager) relative to the $\delta^{13}C$ of dissolved inorganic carbon in Southern Ocean deep water: Implications for glacial ocean circulation models, *Paleoceanography*, *8*(5), 587–610, doi:10.1029/93PA01291.

Mackensen, A., M. Rudolph, and G. Kuhn (2001), Late Pleistocene deep-water circulation in the subantarctic eastern Atlantic, *Global Planet. Change*, *30*, 197–229, doi:10.1016/S0921-8181(01)00102-3.

Matsumoto, K., T. Oba, J. Lynch-Stieglitz, and H. Yamamoto (2002), Interior hydrography and circulation of the glacial Pacific Ocean, *Quat. Sci. Rev.*, *21*, 1693–1704, doi:10.1016/S0277-3791(01)00142-1.

McCorkle, D. C., L. D. Keigwin, B. H. Corliss, and S. R. Emerson (1990), The influence of microhabitats on the carbon isotopic composition of deep-sea benthic foraminifera, *Paleoceanography*, *5*(2), 161–185, doi:10.1029/PA005i002p00161.

Mix, A. C., N. G. Pisias, W. Rugh, J. Wilson, A. Morey, and T. K. Hagelberg (1995), Benthic foraminifer stable isotope record from Site 849 (0–5 Ma): Local and global climate changes, *Proc. Ocean Drill. Program Sci. Results*, *138*, 371–412.

Moore, T. C. Jr., P. D. Rabinowitz, P. E. Borella, N. J. Shackleton, and A. Boersma (1984), History of the Walvis Ridge, *Initial Rep. Deep Sea Drill. Proj.*, *74*, 873–894.

Müller, D. W., D. A. Hodell, and P. F. Ciesielski (1991), Late Miocene to earliest Pliocene (9.8–4.5 Ma) paleoceanography of the subantarctic southeast Atlantic: Stable isotopic, sedimentologic, and microfossil evidence, *Proc. Ocean Drill. Program Sci. Results*, *114*, 459–474.

Murphy, L., D. A. Warnke, C. Andersson, J. Channell, and J. Stoner (2002), History of ice rafting at South Atlantic ODP Site 177-1092 during the Guass and the late Gilbert Chron, *Palaeogeogr. Palaeoclimatol. Palaeoecol.*, *182*, 183–196, doi:10.1016/S0031-0182(01)00495-3.

Ninnemann, U. S., and C. D. Charles (1997), Regional differences in Quaternary subantarctic nutrient cycling: Link to intermediate and deep water ventilation, *Paleoceanography*, *12*(4), 560–567, doi:10.1029/97PA01032.

Ninnemann, U. S., and C. D. Charles (2002), Changes in the mode of Southern Ocean circulation over the last glacial cycle revealed by foraminiferal stable isotopic variability, *Earth Planet. Sci. Lett.*, *201*, 383–396, doi:10.1016/S0012-821X(02)00708-2.

Orsi, A. H., G. C. Johnson, and J. L. Bullister (1999), Circulation, mixing, and production of Antarctic bottom water, *Prog. Oceanogr.*, *43*, 55–109, doi:10.1016/S0079-6611(99)00004-X.

Pagani, M., K. H. Freeman, and M. A. Arthur (1999), Late Miocene atmospheric CO_2 concentrations and the expansion of C_4 grasses, *Science*, *285*, 876–878, doi:10.1126/science.285.5429.876.

Poore, H. R., R. Samworth, N. J. White, S. M. Jones, and I. N. McCave (2006), Neogene overflow of northern component water at the Greenland-Scotland Ridge, *Geochem. Geophys. Geosyst.*, *7*, Q06010, doi:10.1029/2005GC001085.

Raymo, M. E., W. F. Ruddiman, N. J. Shackleton, and D. W. Oppo (1990), Evolution of Atlantic-Pacific $\delta^{13}C$ gradients over the last 2.5 m.y., *Earth Planet. Sci. Lett.*, *97*, 353–368, doi:10.1016/0012-821X(90)90051-X.

Raymo, M. E., D. Hodell, and E. Jansen (1992), Response of deep ocean circulation to initiation of Northern Hemisphere glaciation (3–2 Ma), *Paleoceanography*, *7*(5), 645–672, doi:10.1029/92PA01609.

Shackleton, N. J., and M. A. Hall (1997), The late Miocene stable isotope record, Site 926, *Proc. Ocean Drill. Program Sci. Results*, *154*, 367–373.

Sigman, D. M., M. A. Altabet, R. Francois, D. C. McCorkle, and J.-F. Gaillard (1999), The isotopic composition of diatom-bound nitrogen in Southern Ocean sediments, *Paleoceanography*, *14*(2), 118–134, doi:10.1029/1998PA900018.

Sigman, D. M., S. L. Jaccard, and G. H. Haug (2004), Polar ocean stratification in a cold climate, *Nature*, *428*, 59–63, doi:10.1038/nature02357.

Sigman, D. M., A. M. de Boer, and G. H. Haug (2007), Antarctic stratification, atmospheric water vapor, and Heinrich events: A hypothesis for late Pleistocene deglaciations, in *Past and Future Changes of the Oceanic Meridional Overturning Circulation: Mechanisms and Impacts*, *Geophys. Monogr. Ser.*, vol. 173, edited by A. Schmittner, J. H. C. Chiang, and S. R. Hemming, pp. 335–350, AGU, Washington, D. C.

Stephens, B. B., and R. F. Keeling (2000), The influence of Antarctic sea ice on glacial-interglacial CO_2 variations, *Nature*, *404*, 171–174, doi:10.1038/35004556.

Tedford, R. A., and D. C. Kelly (2004), A deep-sea record of the late Miocene carbon shift from the southern Tasman Sea, in *The Cenozoic Southern Ocean: Tectonics, Sedimentation and Climate Change Between Australia and Antarctica*, *Geophys. Monogr. Ser.*, vol. 151, edited by N. Exon, J. P. Kennett, and M. Malone, pp. 273–290, AGU, Washington, D. C.

Toggweiler, J. R., J. L. Russell, and S. R. Carson (2006), Midlatitude westerlies, atmospheric CO_2, and climate change during the ice ages, *Paleoceanography*, *21*, PA2005, doi:10.1029/2005PA001154.

Venz, K. A., and D. A. Hodell (2002), New evidence for changes in Plio-Pleistocene deep water circulation from Southern Ocean ODP Leg 177 Site 1090, *Palaeogeogr. Palaeoclimatol. Palaeoecol.*, *182*, 197–220, doi:10.1016/S0031-0182(01)00496-5.

Vincent, E., J. S. Killingley, and W. H. Berger (1980), The magnetic epoch-6 carbon shift: A change in the ocean's $^{13}C/^{12}C$ ratio 6.2 million years ago, *Mar. Micropaleontol.*, *5*, 185–203, doi:10.1016/0377-8398(80)90010-9.

Wang, P., J. Tian, X. Cheng, C. Liu, and J. Xu (2004), Major Pleistocene stages in a carbon perspective: The South China Sea record and its global comparison, *Paleoceanography*, *19*, PA4005, doi:10.1029/2003PA000991.

Warnke, D. A., C. P. Allen, D. W. Müller, D. A. Hodell, and C. A. Brunner (1992), Miocene-Pliocene Antarctic glacial evolution as reflected in the sedimentary record: A synthesis of IRD, stable isotope, and planktonic foraminiferal indicators, in *The Antarctic Paleoenvironment: A Perspective on Global Change, Part One*, *Antarct. Res. Ser.*, vol. 56, edited by J. P. Kennett and D. A. Warnke, pp. 311–325, AGU, Washington, D. C.

Watson, A. J., and A. Naveira Garabato (2006), The role of Southern Ocean mixing and upwelling in glacial-interglacial atmospheric CO_2 change, *Tellus, Ser. B*, *58*, 73–87.

Whitworth, T., III, B. A. Warren, W. D. Nowlin Jr., S. B. Rutz, R. D. Pillsbury, and M. I. Moore (1999), On the deep western-boundary current in the southwest Pacific Basin, *Prog. Oceanogr.*, *43*, 1–54, doi:10.1016/S0079-6611(99)00005-1.

I. L. Hendy and T. C. Moore, Department of Geological Sciences, University of Michigan, Ann Arbor, MI 48109, USA.

M. W. Lyle, Department of Oceanography, Texas A&M University, College Station, TX 77843, USA.

L. M. Waddell, Department of Geology, Grand Valley State University, Allendale, MI 49401, USA. (waddelin@umich.edu)